

Nonlinear dielectric response of epitaxial $\text{Ba}_{0.6}\text{Sr}_{0.4}\text{TiO}_3$ thin films

Qing Jiang and Yan-Hong Gao^a

Department of Physics, Suzhou University, Suzhou, 215006, China

Received 4 January 2005

Published online 11 August 2005 – © EDP Sciences, Società Italiana di Fisica, Springer-Verlag 2005

Abstract. Based on Landau-Devonshire (LD)-type phenomenological thermodynamic theory, the electric field dependence of the dielectric properties of tetragonal single-domain barium strontium titanate ($\text{Ba}_{1-x}\text{Sr}_x\text{TiO}_3$) films on cubic substrates is theoretically investigated by taking into account the high order terms of the polarization. At room temperature, the nonlinear dielectric responses of epitaxial $\text{Ba}_{0.6}\text{Sr}_{0.4}\text{TiO}_3$ films are provided by adjusting the film thickness and growth temperature. The strong nonlinearity of relative dielectric constant and pyroelectric coefficient are attained around critical film thickness on MgO (69 nm) and LaAlO_3 (132 nm) substrates or critical growth temperature on MgO (337 °C) substrate with respect to epitaxy-induced lattice misfit and thermal stresses during deposition. This can be explained that small compressive stresses are effective to support high nonlinearity of dielectric constant and pyroelectric coefficient for $\text{Ba}_{0.6}\text{Sr}_{0.4}\text{TiO}_3$ films irrespective of whether they are on compressive substrate or tensile substrate. It is also predicted that a large tunability may be achieved by altering processing conditions, such as the film thickness and growth temperature for different substrates. Our theoretical results are in good agreement with the experimental data reported in literature.

PACS. 77.80.-e Ferroelectricity and antiferroelectricity – 77.80.Bh Phase transitions and Curie point – 77.55.+f Dielectric thin films

1 Introduction

Barium strontium titanate $\text{Ba}_{1-x}\text{Sr}_x\text{TiO}_3$ (BST) films are very attractive dielectric materials because of their unconventional structure and dielectric properties with different composition distribution [1]. In recent years, they have been extensively studied for potential applications of high-density dynamic random access memories (DRAM), electrically tunable microwave devices and pyroelectric detectors. In these devices, large dielectric constant, low dielectric loss and large electric field dependent dielectric properties are required [2,3]. However, nonlinear dielectric response of epitaxial BST thin films is markedly inferior to their bulk sample, which may be attributed to compositional and microstructural inhomogeneities and internal stress [4,5].

Internal stress, as one of the most important factors to determine the quality of epitaxial ferroelectric films materials, originates from mismatch of the lattice parameters and the difference of thermal expansion coefficients (TECs) between substrate and films. The compressive stress appears when substrate lattice parameter is smaller than that of thin films, which means negative signal to strain u_m . On the contrary, the tensile stress occurs and the strain u_m is a positive quantity. With the variation of internal stress, the epitaxial single-domain BST thin films will exhibit different electric and electromechanical

properties. The effect of internal stress on the ferroelectric properties has been profoundly investigated in many theories and experiments. A phenomenological thermodynamic theory provides a more complete description of the intrinsic single domain properties of ferroelectric materials by taking into account actual mechanical boundary conditions. It is theoretically shown that the stress has an important impact on the phase stability and various ferroelectric properties [6]. Pertsev et al. [7] studied that 2D clamping of epitaxial single-domain BaTiO_3 and PbTiO_3 films results in a change in their phase order and gave the “misfit strain-temperature” phase diagram. As a result, five low-temperature phases appear in films comparing with three phases in bulk sample. The “misfit strain-temperature” phase diagrams developed for $\text{Pb}(\text{Zr}_{1-x}\text{Ti}_x)\text{O}_3$ films of different compositions were also presented by Pertsev et al. [8] including the influence of two-dimensional straining and clamping on a “monoclinic gap”. Emelyanov et al. [9] developed the “misfit strain-stress” phase diagrams and considered the effect of external stress on dielectric constant and piezoelectric constant. Experimentally, Taylor et al. [10] pointed that Curie-Weiss temperature decreased with the increase of tensile thermal strain by concerning five different host substrates. Yano et al. [11] reported that the dielectric constant ϵ reaches maximal value at a small stress. Consequently, the strain mechanism is feasible to account for the correlation between the structure and dielectric properties.

^a e-mail: yhgao7@hotmail.com

The total strain of BST films may be relaxed either by domain formation or by further misfit dislocation generation [12]. The latter is related to films thickness at the growth temperature, which means size dependent properties must be considered. Therefore, adjusting the films thickness and selecting appropriate growth temperature are helpful to improve dielectric properties of BST films. With films thickness ranging from 18 nm to 215 nm, the dielectric constant of off-axis sputtered BST films capacitor was far smaller than that of on-axis films because of higher level of in-plane compressive stress at growth temperature 410 °C [13]. Yano et al. [11] showed that the in-plane compressive stress decreased with increasing film thickness in epitaxial BaTiO₃ films on Pt/MgO substrate, which resulted in an increase in the ϵ . The effect of thickness and growth temperature on the temperature dependence of dielectric constant and pyroelectric response of epitaxial films has also been theoretically calculated on various substrates [14,15]. It is shown that the epitaxy-induced negative misfit strain and compressive thermal stress induced *c* phase, which has the polarization vector parallel to [001], in BST films.

A large tunability accompanied by a small dielectric loss is desired to design tunable device. High nonlinear response of dielectric properties is useful to improve the tunability of ferroelectric films. In present paper, our goal is to attain the nonlinear dielectric response of the tetragonal single-domain Ba_{0.6}Sr_{0.4}TiO₃ films on MgO and LaAlO₃ substrates by considering different film thicknesses and growth temperatures. The reason for considering Ba_{0.6}Sr_{0.4}TiO₃ films is that its Curie temperature ($T_c = 5$ °C) is close to room temperature, which may expect a large dielectric constant. Modified thermodynamic theory is used to describe the impact of electric field on the tunability of Ba_{0.6}Sr_{0.4}TiO₃ films. Our theoretical calculation is consistent with experimental results for BST films.

2 Field dependence of dielectric constant

We consider the case of a thin single-domain Ba_{1-x}Sr_xTiO₃ films oriented along [001] with tetragonal [*P4mm*] phase growth on [001] cubic substrate under short-circuit electric boundary condition. The growth temperature T_G is higher than the phase transformation temperature T_C and the film thickness is much smaller than the substrate thickness. For such a configuration, the modified Landau-Devonshire(LD)-type potential can be expressed as [16,17]:

$$F = a_1 P^2 + a_{11} P^4 + a_{111} P^6 - EP + \frac{\{U_m^0 - Q_{12}[P^2 - (P_0^b)^2]\}^2}{S^P}, \quad (1)$$

$$(P_0^b)^2 = \frac{-a_{11} + \sqrt{(a_{11}^2 - 3a_1 a_{111})}}{3a_{111}}. \quad (2)$$

where P_0^b is the spontaneous polarization of the bulk BST; Q_{12} is the electrostrictive coefficient; P is the polarization

of films and E is external electric field alone polarization; $U_m^0 = (b_s - a_f)/b_s$ is misfit strain without considering electric field, where b_s is substrate lattice parameter, a_f is the equivalent cubic cell constant of the free-standing films; $S^P = (S_{11} + S_{12}) - C'$ [17], where S_{ij} are the elastic compliances, C' is a constant which is determined by the piezomodulus and dielectric susceptibility of unstressed films; a_1 is the dielectric stiffness and is in accordance with Curie-Weiss law, i.e., $a_1 = \frac{T-T_0}{2\epsilon_0 C}$, T_0 and C are the Curie-Weiss temperature and constant of a bulk ferroelectric, respectively, and ϵ_0 is the permittivity of free space; a_{11} , a_{111} are higher order stiffness coefficients at constant stress. By averaging the corresponding parameters of BaTiO₃ and SrTiO₃, the parameters of Ba_{0.6}Sr_{0.4}TiO₃ films in calculation are given in Table 1 [7,14,18]. The potential in equation (1) can be renormalized by modifying the coefficients:

$$F = \frac{1}{2} a_1^* P^2 + \frac{1}{4} a_{11}^* P^4 + \frac{1}{6} a_{111}^* P^6 - EP + \frac{[U_m^0 + Q_{12}(P_0^b)^2]^2}{S^P}, \quad (3)$$

The modified coefficients are given by:

$$a_1^* = 2 \left(a_1 - \frac{2[U_m^0 + Q_{12}(P_0^b)^2]^2 Q_{12}}{S^P} \right), \quad (4)$$

$$a_{11}^* = 4 \left(a_{11} + \frac{Q_{12}^2}{S^P} \right), \quad (5)$$

$$a_{111}^* = 6a_{111}. \quad (6)$$

According to equation (3), the expression for spontaneous polarization P_0^f of constrained films can be derived from the potential function using the stability criterion of the first derivative $(dF/dP)|_{E=0} = 0$:

$$a_1^* P + a_{11}^* P^3 + a_{111}^* P^5 - E = 0. \quad (7)$$

Then the polarization with zero electric field can be obtained:

$$P_0^f = \sqrt{\frac{(a_{11}^{*2} - 4a_1^* a_{111}^*)^{1/2} - a_{11}^*}{2a_{111}^*}}. \quad (8)$$

The field induced polarization is defined as

$$p = P - P_0^f. \quad (9)$$

In order to consider nonlinear response, substituting equation (9) into equation (7) and taking into account the third-order terms of p , equation (7) can be simplified as:

$$E = \alpha_1 p + \alpha_2 p^2 + \alpha_3 p^3, \quad (10)$$

where

$$\alpha_1 = a_1^* + 3a_{11}^* (P_0^f)^2 + 5a_{111}^* (P_0^f)^4, \quad (11)$$

$$\alpha_2 = 3a_{11}^* P_0^f + 10a_{111}^* (P_0^f)^3, \quad (12)$$

$$\alpha_3 = a_{111}^* + 10a_{111}^* (P_0^f)^2. \quad (13)$$

Table 1. The parameters of Ba_{0.6}Sr_{0.4}TiO₃ films used to calculate modified coefficients. (T_c : Curie temperature, C : Curie constant, a_{ij} and a_{ijk} : stiffness coefficients, S_{ij} : elastic compliances, Q_{ij} : electrostrictive coefficient. The temperature T in °C).

parameter	Ba _{0.6} Sr _{0.4} TiO ₃
T_c (°C)	5
C (°C)	1.22×10^5
a_{11} (m ⁵ /C ² F)	$(2.16T + 462) \times 10^6$
a_{111} (m ⁹ /C ⁴ F)	6.6×10^9
S_{11} (m ² /N)	5.12×10^{-12}
S_{12} (m ² /N)	-1.65×10^{-12}
Q_{12} (m ⁴ /C ²)	-0.034

So, the electric field dependence of susceptibility is presented as

$$\chi^f(E) = \frac{1}{\varepsilon_0} \frac{dp}{dE} = \frac{3\alpha_3 \left[-2\alpha_2^2 + 6\alpha_1\alpha_3 + (2\lambda_2^2)^{1/3} \right]}{\varepsilon_0 \lambda_1 (4\lambda_2)^{1/3}}, \quad (14)$$

where

$$\lambda_1 = \left[-4(\alpha_2^2 - 3\alpha_1\alpha_3)^3 + (-2\alpha_2^3 + 9\alpha_1\alpha_2\alpha_3 + 27\alpha_3^2 E)^2 \right]^{1/2}, \quad (15)$$

$$\lambda_2 = -2\alpha_2^3 + 9\alpha_1\alpha_2\alpha_3 + 27\alpha_3^2 E + \lambda_1, \quad (16)$$

and ε_0 is the dielectric susceptibility of vacuum.

Then, the relative dielectric constant ε is derived from:

$$\frac{1}{\varepsilon} = \frac{1}{1 + \chi^f(E)}. \quad (17)$$

In epitaxial BST films, the film thickness h has a great effect on the internal strains due to the relaxation of lattice misfit-induced stresses by the formation of misfit dislocations. At growth temperature T_G , the equilibrium linear misfit dislocation density ρ is written as [12, 19]

$$\rho = \frac{u_m(T_G)}{a_f(T_G)} \left(1 - \frac{h_c}{h} \right), \quad (18)$$

where $u_m(T_G)$ and $a_f(T_G)$ are the effective misfit strain and film lattice parameter at growth temperature T_G ; h_c means the critical thickness below which the generation of misfit dislocation is not feasible. Assuming no additional dislocations form during cooling down, the “effective” substrate lattice parameter b_s^* can be defined by

$$b_s^*(T) = \frac{b_s(T)}{\rho b_s(T) + 1}, \quad (19)$$

where $b_s(T)$ is substrate lattice parameter at temperature T . Therefore, the misfit strain of the films U_m^0 at any temperature may be calculated according to above equation instead of actual lattice parameter b_s if the substrate lattice parameter is given as a function of temperature.

$$U_m^0(T) = \frac{b_s^*(T) - a_f(T)}{b_s^*(T)}. \quad (20)$$

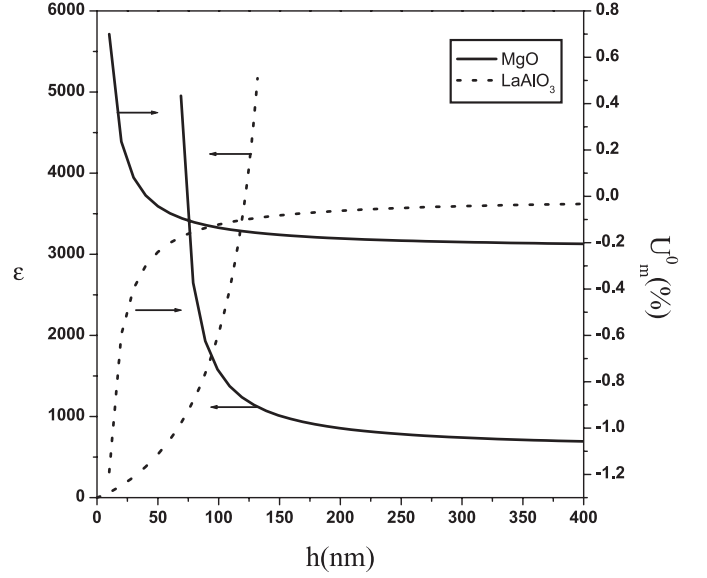


Fig. 1. At zero electric field, the thickness dependence of relative dielectric constant and misfit strain for different substrates.

Table 2. Lattice parameters of Ba_{0.6}Sr_{0.4}TiO₃ films and substrates at RT and their respective TECs.

	Lattice parameters(nm)	TEC(°C)
Ba _{0.6} Sr _{0.4} TiO ₃	0.3960	10.5×10^{-6}
MgO	0.4211	13.47×10^{-6}
LaAlO ₃	0.3787	10.0×10^{-6}

To study the nonlinear response of dielectric constant for Ba_{0.6}Sr_{0.4}TiO₃ films with the variation of film thickness at room temperature(RT) $T = 25$ °C, we chose MgO and LaAlO₃ substrates. Compared with Ba_{0.6}Sr_{0.4}TiO₃ films lattice parameter, MgO is tensile substrate and LaAlO₃ is compressive substrate. The lattice parameters at RT and thermal expansion coefficients(TECs) are listed in Table 2 [14, 20]. In calculation, we take $T_G = 800$ °C. Accordingly, the $u_m(T_G)$, h_c are calculated to be 6.195%, 1.5 nm for MgO substrate and -4.57%, 2.6 nm for LaAlO₃ substrate, respectively [21]. The lattice parameter of Ba_{0.6}Sr_{0.4}TiO₃ films is 0.3964 nm at growth temperature T_G [22]. The uncertainty in elastic compliance is less important in determining the nonlinear response compared to the effect of misfit [16]. For comparison with experimental data, we estimate that S^P is 2.5×10^{-12} m²N⁻¹.

At zero electric field, the film thickness dependence of relative dielectric constant and misfit strain is plotted in Figure 1 for different substrates. With the increase of Ba_{0.6}Sr_{0.4}TiO₃ films thickness, the misfit strain may be relaxed completely because of the configuration of misfit dislocation, which is not only for tensile substrate but also for compressive substrate. Significantly, the misfit strain may vary from tensile strain to compressive strain on MgO substrate. According to the phase diagram [14], the compressive strain is beneficial to stable tetragonal phase. At room temperature(RT), the phase

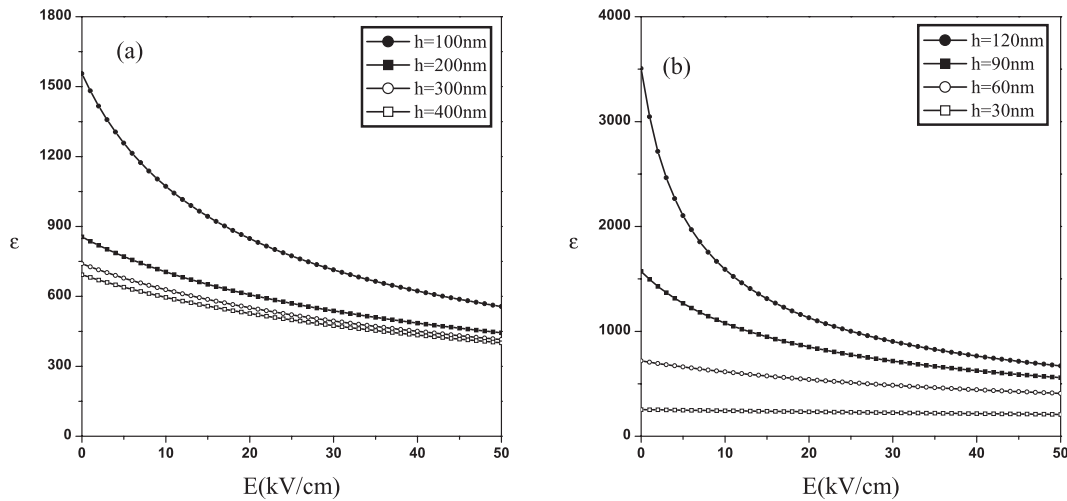


Fig. 2. The relative dielectric constant nonlinear response of $\text{Ba}_{0.6}\text{Sr}_{0.4}\text{TiO}_3$ epitaxial films (a) on MgO substrate, (b) on LaAlO_3 substrate.

transformation of $\text{Ba}_{0.6}\text{Sr}_{0.4}\text{TiO}_3$ films takes place from paraelectric phase to tetragonal phase when the misfit stress $U_m^0(RT) = -0.094\%$. Taking into account the formation of misfit dislocation in thin films, this value of misfit stress corresponds to different film thickness when films grow on different substrates. Using equations (18–20), we obtain that the critical film thickness of $\text{Ba}_{0.6}\text{Sr}_{0.4}\text{TiO}_3$ films with misfit stress -0.094% is 69 nm on MgO substrate and 132 nm on LaAlO_3 substrate, respectively. Comparing relationship between misfit stress and film thickness, showed in Figure 1, with phase diagram [14], we find that the ferroelectric tetragonal phase is stable when the film thickness of $\text{Ba}_{0.6}\text{Sr}_{0.4}\text{TiO}_3$ is greater than 69 nm on MgO substrate, and smaller than 132 nm on LaAlO_3 substrate. Vice versa, the paraelectric phase favors. This kind of behavior is quite similar to film size effect, i.e., size driving phase transformation. In our following discussion, we select a suitable thickness to make $\text{Ba}_{0.6}\text{Sr}_{0.4}\text{TiO}_3$ films to be in tetragonal phase both on MgO and LaAlO_3 substrates. Figure 1 also shows the behavior of dielectric constant of $\text{Ba}_{0.6}\text{Sr}_{0.4}\text{TiO}_3$ ferroelectric films on different substrates with film thickness. The dielectric constants disperse at the film thickness being 67 nm on MgO substrate and 132 nm on LaAlO_3 substrate. It is meaningful that the dielectric constant reaches maximal value at small compressive stress both tensile and compressive substrates, and decreases when compressive stress increases, which is accordance with experimental results [11, 13].

In order to understand the nonlinear response of dielectric constant, according to equation (12), the relative dielectric constant ϵ as a function of external electric field is exhibited in Figure 2. Figure 2a represents the case of $\text{Ba}_{0.6}\text{Sr}_{0.4}\text{TiO}_3$ films deposited on MgO substrate. As can be seen, the dielectric constant shows almost linear relationship with external electric field for thicker films, such as 400 nm. With the decrease of film thickness, the nonlinear response of dielectric constant is improved within a certain range of electric field. It's remarkable that the

strong nonlinearity of electric field dependence of dielectric constant may be observed around critical film thickness 69 nm, for example 100 nm. According to Figure 1, the phenomenon can be explained that small compressive strain supports the formation of dramatic nonlinearity. The $\text{Ba}_{0.6}\text{Sr}_{0.4}\text{TiO}_3$ films deposited on LaAlO_3 substrate is presented in Figure 2b. The less electric field dependence of dielectric constant is shown when $\text{Ba}_{0.6}\text{Sr}_{0.4}\text{TiO}_3$ film thickness is far away from critical thickness 132 nm. With the increase of film thickness, the nonlinear response of dielectric constant is intensified and the strong nonlinear response appears near critical thickness 132 nm, for example 120 nm. Consequently, the high nonlinearity of dielectric constant may be obtained under small compressive strains for $\text{Ba}_{0.6}\text{Sr}_{0.4}\text{TiO}_3$ films irrespective of whether they are under compressive substrate or tensile substrate. The nonlinear response is lowered with the increase in the magnitude of misfit strain. In practice, for nonlinear response of dielectric constant, it is important to consider the critical film thickness for different substrates. Obviously, nonlinear dielectric response is strongly film thickness dependent. We noticed that some previous works [23–25] have already take the thickness dependence of dielectric constant into account. A variety of mechanisms being invoked to explain this behavior are summarized in reference [25]. In our present model, the effect of film thickness on dielectric response is considered by forming misfit dislocation in thin films, and can be classified as one of the intrinsic mechanism.

Figure 3 predicts the tunability of $\text{Ba}_{0.6}\text{Sr}_{0.4}\text{TiO}_3$ films on MgO and LaAlO_3 substrates as a function of film thickness with an applied electric field $E = 40$ kV/cm. In tetragonal phase, the tunability is calculated by $[\epsilon(0) - \epsilon(E)]/\epsilon(0) \times 100\%$. It is clearly seen that the maximum in tunability reaches 83.7% and 84.3% at critical film thickness 69 nm and 132 nm on MgO and LaAlO_3 substrates, respectively. According to Figure 1, the maximum is ascribed to a phase transformation from tetragonal phase to paraelectric phase. With the

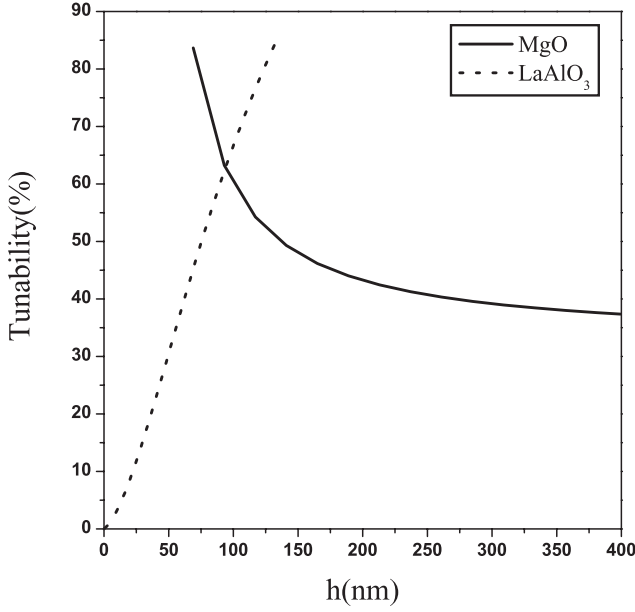


Fig. 3. The tunability of Ba_{0.6}Sr_{0.4}TiO₃ films on MgO and LaAlO₃ substrates as a function of film thickness with an applied electric field $E = 40$ kV/cm.

increase of film thickness, the tunability slowly decreases to 35% on MgO substrate. However, the tunability increases monotonously on LaAlO₃ substrate. These mean that the small compressive stress is helpful to develop high tunability in tetragonal phase.

To provide the effect of the thermal stresses, which result from the difference in TECs between the films and the underlying substrates, on nonlinear response of Ba_{0.6}Sr_{0.4}TiO₃ films, we assume the grain size D is equal to or smaller than the film thickness h so that internal stresses are relatively small and can be neglected. As the films are cooled from growth temperature T_G , the thermal stresses dominate. We take $U_{thermal}$ as a function of temperature [10,26]:

$$U_{thermal} = \int_T^{T_G} (\alpha_{film} - \alpha_{substrate}) dt \quad (21)$$

where α_{film} and $\alpha_{substrate}$ are the TECs of the films and substrates, respectively. In calculation, U_m^0 is substituted by $U_{thermal}$. From Table 2, we find that the difference of TECs between Ba_{0.6}Sr_{0.4}TiO₃ films and LaAlO₃ substrate is so small that the effect of the thermal stresses on LaAlO₃ substrate can be neglected. In other words, the epitaxial Ba_{0.6}Sr_{0.4}TiO₃ films on LaAlO₃ substrate is only in cubic paraelectric phase if growth temperature is below 2000 °C. Therefore, we only consider the effect of the thermal stresses on MgO substrate in this paper.

On MgO substrate, the influence of growth temperature T_G on the dielectric constant and misfit strain is shown in Figure 4 with zero external electric field. The misfit strain is always compressive thermal strain in the range of considering growth temperature. It means that Ba_{0.6}Sr_{0.4}TiO₃ films are always in the paraelectric phase or the tetragonal ferroelectric phase basing on

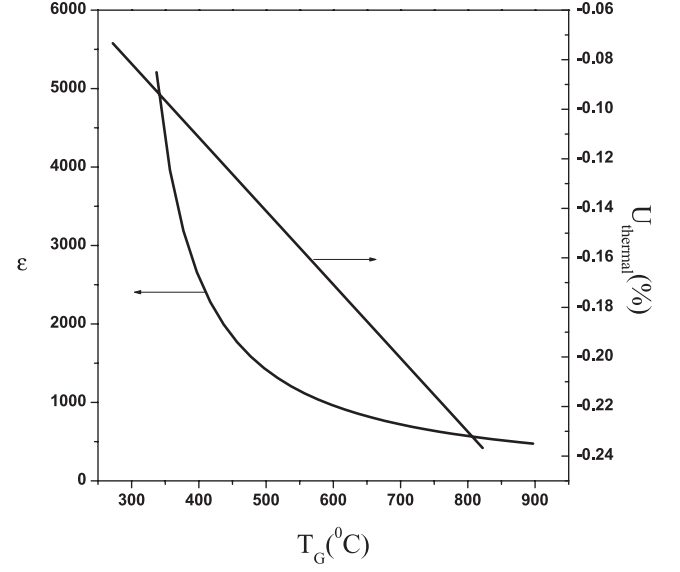


Fig. 4. On MgO substrate, the influence of growth temperature T_G on relative dielectric constant and misfit strain with zero external electric field.

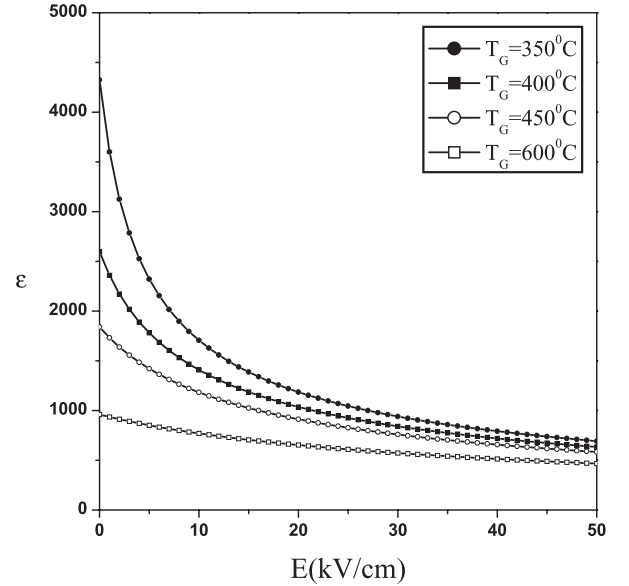


Fig. 5. The external electric field dependence of the relative dielectric constant ϵ for different growth temperatures on MgO substrate.

“temperature-misfit strain” phase diagram [14]. To ensure the epitaxial Ba_{0.6}Sr_{0.4}TiO₃ films exist in tetragonal ferroelectric phase, the growth temperature must exceed 337 °C. With the enhancement of the growth temperature, the magnitude of compressive strain linearly increases resulting in the decrease of relative dielectric constant.

Figure 5 exhibits the external electric field dependence of the relative dielectric constant ϵ for different growth temperatures on MgO substrate. With lowering the growth temperature, the relative dielectric constant increases and the dielectric nonlinearity improves. The strong dielectric nonlinearity is seen at growth temperature 350 °C that is in the vicinity of critical growth

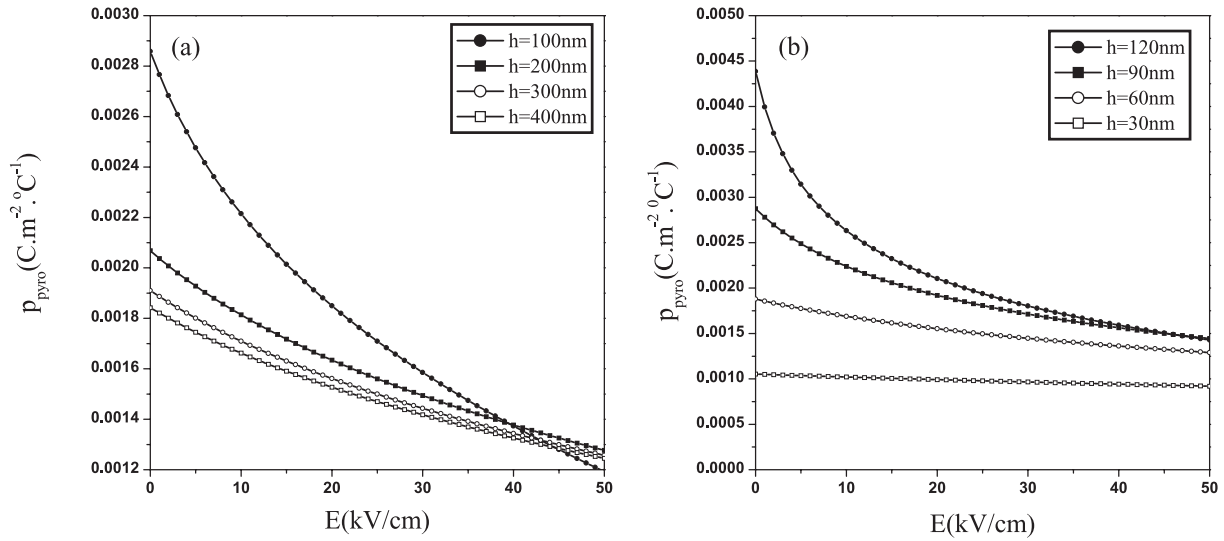


Fig. 6. The external electric field dependence of pyroelectric coefficient (a) on MgO substrate (b) on LaAlO₃ substrate with various film thicknesses.

temperature 337 °C. We believe that the dielectric constant tunability can greatly increase at a relatively low growth temperature ($T_G > 337$ °C) when epitaxial Ba_{0.6}Sr_{0.4}TiO₃ films are deposited on MgO substrate.

3 Field dependence of pyroelectric coefficient

The pyroelectric coefficient p_{pyro} of BST films along [001]-direction in tetragonal phase is given as the sum of the derivation of the spontaneous polarization P_0^f and the field induced polarization p with the temperature:

$$p_{pyro} = -\frac{\partial P}{\partial T} = -\frac{\partial P_0^f}{\partial T} - \frac{\partial p}{\partial T}. \quad (22)$$

According to equation (18-22), we can obtain the effect of film thickness and growth temperature on nonlinear response of pyroelectric coefficient.

To study the pyroelectric response of different substrates with the change of Ba_{0.6}Sr_{0.4}TiO₃ film thickness, we consider the growth temperature T_G is 800 °C. On MgO substrate, the external electric field dependence of pyroelectric coefficient is displayed in Figure 6a with various film thicknesses. The pyroelectric coefficient is approximal to 0.00184C/m².°C-0.0019C/m².°C for thicker films ($h \geq 300$ nm) at zero electric field, which are in good agreement with experimental data of 0.0018C/m².°C [27]. The pyroelectric response linearly decreases with the increase of external electric field when films are thicker than 300 nm. The pyroelectric nonlinearity appears for thinner films, and strong nonlinearity can be seen close to critical film thickness because of structural transformation. We can obtain the maximum of pyroelectric coefficient around critical thickness without external electric field. However, for thicker films, the pyroelectric coefficient values exceed that of thinner films when applied field increases successively. Figure 6b shows the pyroelectric response on

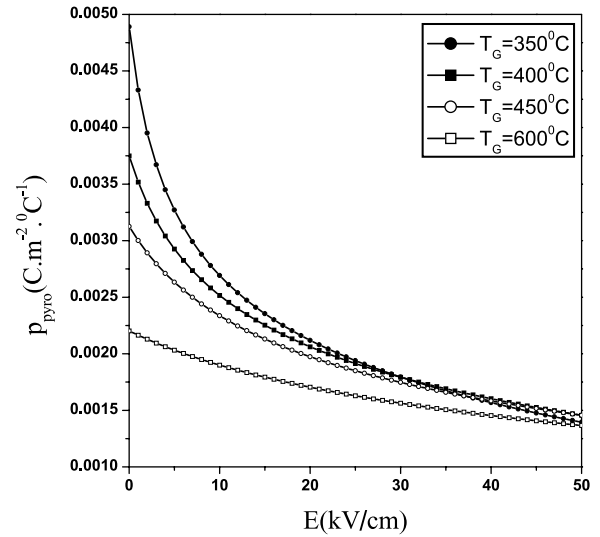


Fig. 7. The pyroelectric coefficient as a function of external electric field with various growth temperatures on MgO substrate.

LaAlO₃ substrate with different film thicknesses. The impact of film thickness on pyroelectric nonlinearity is opposite to that of Ba_{0.6}Sr_{0.4}TiO₃ films deposited on MgO substrate. If the film thickness is much smaller than critical film thickness, the pyroelectric coefficient is almost invariable with the increase of external electric field.

At RT, the pyroelectric coefficient as a function of external electric field is presented in Figure 7 with various growth temperatures on MgO substrate. It is clear that the pyroelectric nonlinear response of Ba_{0.6}Sr_{0.4}TiO₃ films improves with the decrease of growth temperature, and obvious pyroelectric nonlinearity is observed around critical growth temperature because the small compressive stresses induce ferroelectric-paraelectric phase transition.

4 Conclusions

In summary, a theoretical formalism has been used to investigate the combined effect of film thickness and growth temperature on nonlinear response of electric field dependence of dielectric and pyroelectric properties for the tetragonal single-domain Ba_{0.6}Sr_{0.4}TiO₃ epitaxial films with different growth substrates. Quantitative calculations show that both lattice misfit and thermal stresses have important influence on the dielectric constant and pyroelectric nonlinear response. When film thickness is far away from critical film thickness, the dielectric constant and pyroelectric coefficient of Ba_{0.6}Sr_{0.4}TiO₃ epitaxial films almost have a linear relationship with the electric field. However, the dramatic nonlinear response can be observed near critical film thickness, such as 100 nm for MgO substrate and 120 nm for LaAlO₃ substrate. It can be explained that small compressive stresses are effective to high nonlinearity of dielectric constant and pyroelectric coefficient irrespective of compressive substrate or tensile substrate. In addition, the critical growth temperature can greatly improve the nonlinearity of dielectric constant and pyroelectric coefficient of Ba_{0.6}Sr_{0.4}TiO₃ epitaxial films because of the small thermal compressive stresses. A large tunability is also predicted at critical film thickness in present paper. It can be actually practical to obtain high dielectric and pyroelectric tunability of epitaxial Ba_{0.6}Sr_{0.4}TiO₃ films by adjusting the film thickness and the deposition temperature.

This work was supported by the National Natural Science Foundation of China under the Grant No.10374069, Jiangsu provincial Natural Science Foundation under the Grant No.BK2003032, and Jiangsu Key Laboratory of Film Materials of China.

References

1. Y. Gim, T. Hudson, Y. Fan, C. Kwon, A.T. Findikoglu, B.J. Gibbons, B.H. Park, Q.X. Jia, *Appl. Phys. Lett.* **77**, 1200 (2000)
2. B. Nagaraj, T. Sawhney, S. Perusse, S. Aggarwal, R. Ramesh, V.S. Kaushik, S. Zafar, R.E. Jones, J.H. Lee, V. Balu, J. Lee, *Appl. Phys. Lett.* **74**, 3194 (1999)
3. C.S. Hwang, S.O. Park, H.J. Cho, C.S. Kang, H.K. Kang, S.I. Lee, M.Y. Lee, *Appl. Phys. Lett.* **67**, 2819 (1995)
4. J. Im, O. Auciello, P.K. Baumann, S.K. Streiffer, D.Y. Kaufman, A.R. Krauss, *Appl. Phys. Lett.* **76**, 625 (2000)
5. W. Chang, C.M. Gilmore, W.J. Kim, J.M. Pond, S.W. Kirchoefer, S.B. Qadri, D.B. Chirsey, J.S. Horwitz, *J. Appl. Phys.* **87**, 3044 (2000)
6. S.H. Oh, H.M. Jang, *Phys. Rev. B.* **62**, 14757 (2000)
7. N.A. Pertsev, A.G. Zembilgotov, A.K. Tagantsev, *Phys. Rev. Lett.* **80**, 1988 (1998)
8. N.A. Pertsev, V.G. Kukhar, H. Kohlstedt, R. Waser, *Phys. Rev. B.* **67**, 054107 (2003)
9. A.Y. Emelyanov, N.A. Pertsev, A.L. Kholkin, *Phys. Rev. B.* **66**, 214108 (2002)
10. T.R. Taylor, P.J. Hansen, B. Acikel, N. Pervez, R.A. York, S.K. Streiffer, J.S. Speck, *Appl. Phys. Lett.* **80**, 1978 (2002)
11. Y. Yano, K. Lijima, *J. Appl. Phys.* **76**, 7833 (1994)
12. J.S. Speck, W. Pompe, *J. Appl. Phys.* **76**, 466 (1994)
13. W.Y. Park, K.H. Ahn, C.S. Hwang, *Appl. Phys. Lett.* **83**, 4387 (2003)
14. Z.G. Ban, S.P. Alpay, *J. Appl. Phys.* **91**, 9288 (2002)
15. A. Sharma, Z.G. Ban, S.P. Alpay, J.V. Mantese, *J. Appl. Phys.* **95**, 3618 (2004)
16. L. Chen, V. Nagarajan, R. Ramesh, A.L. Roytburd, *J. Appl. Phys.* **94**, 5147 (2003)
17. A.L. Roytburd, S.P. Alpay, V. Nagarajan, C.S. Ganpule, S. Aggarwal, E.D. Williams, R. Ramesh, *Phys. Rev. Lett.* **85**, 190 (2000)
18. N.A. Pertsev, A.K. Tagantsev, N. Setter, *Phys. Rev. B.* **61**, R825 (2000)
19. S.P. Alpay, A.L. Roytburd, *J. Appl. Phys.* **83**, 4714 (1998)
20. W. Chang, J.S. Horwitz, A.C. Carter, J.M. Pond, S.W. Kirchoefer, C.M. Gilmore, D.B. Chirsey, *Appl. Phys. Lett.* **74**, 1033 (1999)
21. J.W. Matthews, A.E. Blakeslee, *J. Cryst. Growth.* **27**, 118 (1974)
22. B.H. Park, Y. Gim, Y. Fan, Q.X. Jia, P. Lu, *Appl. Phys. Lett.* **77**, 2587 (2000)
23. U. Ellerkmann, R. Liedtke, U. Boettger, R. Waser, *Appl. Phys. Lett.* **85**, 4708 (2004)
24. C. Basceri, S.K. Streiffer, A.I. Kingon, R. Waser, *J. Appl. Phys.* **82**, 2497 (1997)
25. S.K. Streiffer, C. Basceri, C.B. Parker, S.E. Lash, A.I. Kingon, *J. Appl. Phys.* **86**, 4565 (1999)
26. R.W. Hoffman, *Thin Solid Films* **34**, 185 (1976)
27. T.J. Zhang, H. Ni, *Sens. Actuators A* **100**, 252 (2002)